LARGE AREA POINT CLOUD BASED SOLAR RADIATION MODELING

ANDREAS JOCHEM [1,2], VOLKER WICHMANN [1,3], BERNHARD HÖFLE [4]

[1]alpS-Centre for Climate Change Adaptation Technologies, Grabenweg 3, 6020 Innsbruck, Austria, (jochem@alps-gmbh.at)

[2] University of Innsbruck, Department of Geography, 6020 Innsbruck, Austria

[3] Laserdata GmbH-Management and Analysis of Laserscanning Data, 6020 Innsbruck, Austria

[4] University of Heidelberg, Department of Geography, Chair of GIScience, 69120 Heidelberg, Germany

Abstract: Most solar radiation models implemented in Geographical Information Systems (GIS) operate on 2.5D raster data. There are only a few models using the full 3D information of a point cloud obtained by e.g. Airborne Laser Scanning (ALS) systems. However, models performing point cloud based solar radiation modeling are not suitable for large study areas because the huge amount of point cloud data cannot be handled in one go in the computer's main memory. Deconstructing the whole dataset into several tiles requires the usage of buffer areas surrounding each tile to avoid edge effects when calculating necessary features such as slope and aspect as well as shadowing effects of nearby objects within the point cloud. In this paper a point cloud based solar radiation model that is fully implemented in SAGA GIS is presented and applied to large areas.

1 INTRODUCTION

The incoming solar radiation is the primary source of energy that directly influences many biological, physical and biophysical processes. Furthermore, it is the basic resource for solar based renewable energy technologies such as solar thermal or photovoltaic conversion systems (Myers 2003). Hence having knowledge of the amount of the incoming solar radiation on the Earth's surface at various geographic locations is interesting in ecological (e.g. agriculture, forestry, meteorology) as well as in economic (e.g. finding suitable areas for the installation of solar based renewable energy technologies) terms. Most solar radiation models implemented in Geographical Information Systems (GIS) operate on 2.5D raster data (Fu and Rich 1999; Fu and Rich 2002; Pons and Ninyerola 2008). The usage of such models in combination with 3D point cloud (xyz-triples) data obtained by e.g. Airborne Laser Scanning (ALS) systems (Wehr and Lohr 1999), also referred to as Light Detection And Ranging (LiDAR), is not given and requires an aggregation and simplification of the 3D point cloud to 2.5D raster cells (Kassner et al. 2008; Vögtle et al. 2005; Ludwig et al. 2009). This procedure drastically reduces the storage size of the point cloud data and makes processing less time consuming because the complexity of the 3D space has not to be considered anymore. However, the 3D information is irreversibly lost because all 3D shapes such as caves or overhangs cannot be represented in 2.5D raster data, because for each planimetric (x,y) position, only one height (z) is admissible, meaning that the surface is represented by a single-valued function. Due to the fact that slope, aspect and shadowing effects may vary at each point strong local gradients in the incoming solar radiation may occur. These gradients can be modeled in a more detailed way by performing solar radiation modeling on the original 3D point cloud and taking its 3rd dimension into account.

There are only a few models using the full 3D information of a point cloud. Jochem et al. (2009a) segment a 3D point cloud obtained by ALS Systems into homogeneous areas fulfilling the defined constraints of roof planes. Solar radiation modeling is performed on each point of each detected roof plane. Shadowing effects of nearby objects are taken into account by calculating the horizon of each point within the point cloud. A further study (Jochem et al. 2009b) considered transparent properties of vegetation by introducing transparent shadow values for detected vegetation objects. However, those point cloud based solar radiation models are not suitable for large study areas because the huge amount of point cloud data cannot be handled in one go in the computer's main memory. A workflow handling a huge amount of point cloud data is described in He (2010). The author presents a method for automatic extraction of Digital Terrain Models (DTM) from ALS Data by splitting the whole dataset into several small overlapping tiles.

The objective of this paper is to use a previously developed point cloud based solar radiation model and apply it to a large study area (7 km x 7 km). The presented model is completely implemented in SAGA GIS[1], which allows the use of its *Point Cloud* data type and its processing tools. The model considers shadowing as well as atmospheric effects. In order to take the limitation of the computer's main memory into account the whole point cloud data set is managed within a Laser data Information System (Höfle 2007; Petrini-Monteferri et al. 2009) and decomposed into small subareas for processing.

This paper is structured as follows: In Section 2 the study area and the available ALS datasets are presented. The methodology including point feature calculation and the creation of overlapping tiles is described in Section 3. The point cloud based solar radiation model, the calculation of shadowing effects and its application are subject of Section 4. The results are presented and discussed in Section 5. A conclusion and outlook on future works are given in Section 6.

2 STUDY AREA AND DATASETS

Test site and data acquisition

The investigated study area is part of the city of Feldkirch in the Federal state of Vorarlberg (Austria) and covers an area of about 7 km x 7 km. Besides built-up areas, which are mainly characterized by single houses and block buildings, the study area consists of different land cover types such as forests and agricultural land. Additionally, the study area contains small structures like cars, fences and single vegetation objects of different geometry and type.

The airborne LiDAR data were acquired under snow-free conditions in the framework of a commercial Vorarlberg-wide terrain mapping campaign in the years 2002 to 2004. The used Leica ALS-50 scanner has a wavelength of 1064 nm, a pulse repetition frequency of 57 kHz, a maximum swath width of 75° and both first and last echoes were recorded. The average point density within the area of Feldkirch is 17 points/m² (Rieger et al. 2005), resulting in 833 x 10^6 points in total.

1 *http://www.saga-gis.org*

Data management

The whole point cloud dataset is stored in a Laser data Information System (LIS) based on a PostgreSQL/PostGIS[2] database (Petrini-Monteferri et al. 2009). It was developed based on the scientific findings of Höfle (2007) and allows seamless spatial queries on point clouds as well as updating and adding of point cloud attributes. The results of the solar radiation calculations can be stored either in the SAGA GIS *Point Cloud* data type or within the LIS database.

3 METHODOLOGY

Workflow

The whole point cloud dataset is divided into small subareas, i.e. into tiles, to overcome the limitation of the computer's main memory. A buffer area is assigned to each tile. This procedure avoids edge effects when calculating necessary features such as slope and aspect as well as shadowing effects of nearby objects within the point cloud. As shown in Figure 1 each tile is treated separately. The presented point cloud based operations (feature calculation, modeling of nearby shadows) require information about the local neighborhoods of the points i.e. finding the *k* nearest neighbors and the fixed distance neighbors, respectively, of each point. In this study these operations are performed by making use of the approximate nearest neighbors library (ANN) (Mount and Arya 1997). ANN based algorithms are completely executed in the computer's main memory. Hence, tiling of large point cloud datasets i.e. dividing the data into smaller tasks is required. Therefore, a special SAGA Module was developed to retrieve the point cloud data within each tile from the database and process it within SAGA GIS. Detailed descriptions of each step shown in Figure 1 are given below.

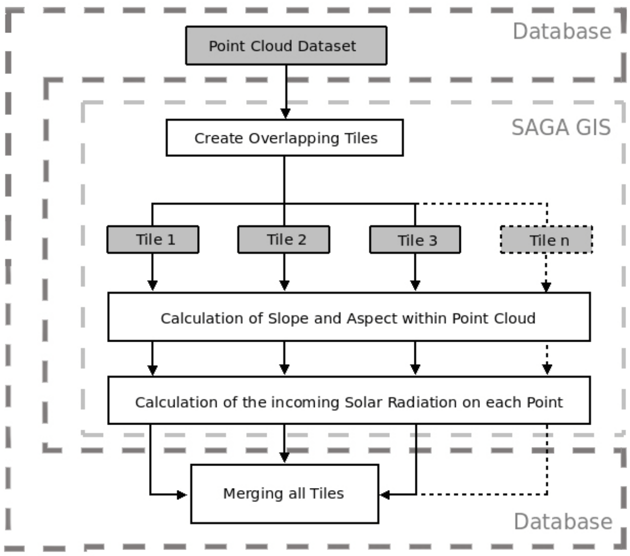

Fig. 1: Workflow for seamless point cloud based solar radiation assessment.

Creation of overlapping tiles

ALS mapping projects usually cover large areas (typically >500 km²) and are stored as an

2 *http://postgis.refractions.net*

unorganized set of 3D points (xyz-triples). This leads to a huge amount of data exceeding the memory of common computer hardware. Therefore, the whole dataset has to be divided into several tiles with similar size, whereas the size of each tile depends on the size of the memory (e.g. max. 4 GB) (He 2010). This procedure is performed in 2D and is based on the x and y coordinate information of the point cloud. Point features such as slope and aspect are computed by taking the 3D *k* nearest neighbors (e.g. *k*=17) of the point of interest into account (Section 3.3). Therefore, a buffer area is assigned to each tile in order to guarantee a proper selection of the *k* nearest neighbors in regions being close to the edge of a tile. Additionally, such buffer areas are also required for correct calculations of shadowing effects of nearby objects (Section 4.2). The creation of overlapping tiles is illustrated in Figure 2. Each tile overlaps its adjacent tiles. The tiles are represented in black bold squares. The striped areas represent the buffer areas of each tile.

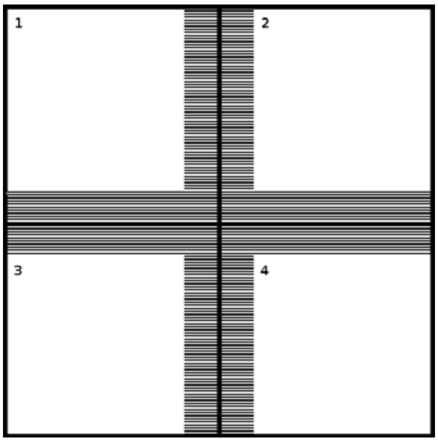

Fig 2: Creation of overlapping tiles

Point based calculation of slope and aspect

The determination of slope and aspect of each point is of fundamental importance to perform point cloud based solar radiation modeling. The slope of a point is defined as the angle between the horizontal plane (xy-plane) and the orthogonal regression plane that is fitted to the point of interest and its 3D *k* nearest neighbors (*k*>2). The angle between two planes is given by the angle between the normal vectors. The aspect of each point is determined by projecting the normal vector of the fitted orthogonal regression plane on the xy-plane and calculating the angle (clockwise) from the y-axis representing the North direction.

4 SOLAR RADIATION MODELING

Background

In this paper a previously developed point cloud based solar radiation model is presented that estimates the incoming global solar radiation by considering atmospheric and shadowing effects (Jochem et al. 2009a; Jochem et al. 2009b). The global radiation is computed as the sum of the direct and diffuse radiation. Formulas estimating both components are taken from Hofierka and Šúri (2002). The position of the sun at any time and its incidence angle on the point of interest are calculated by using the SOLPOS Code developed by the National Renewable Energy Laboratory (NREL 2002). Data from a nearby meteorological ground station is used to calculate the clear sky index (CSI) in order to correct the modeled incoming global radiation and consider atmospheric as well as shadowing effects of the terrain (i.e. shadows casted by mountains and hills, respectively). On horizontal locations the CSI is defined as the ratio of the radiation that is observed at meteorological stations and the modeled global radiation. Inclined locations have a different ratio of direct and diffuse radiation. Therefore, the CSI has to be computed for both the direct and the diffuse component of the global radiation. In this study the CSI is computed for horizontal surfaces only and is also applied on inclined locations, due to lack of reference data from meteorological stations. Modeled values are corrected by multiplication with the CSI. Detailed information on the CSI can be found in e.g. Šúri & Hofierka (2004).

Shadowing effects

The presented model considers both shadows of nearby objects and shadows of the surrounding terrain (mountains, hills). It is assumed that shadows of nearby objects have the greatest influence on the strong local gradients in the incoming solar radiation. Therefore, these shadows have to be modeled in a proper way by using the full 3D information of the point cloud and calculating the 3D horizon of each point within a defined distance (e.g. 60 m). The modeling of the horizon is performed by determining the minimum solar elevation angle for each azimuth direction (i.e. the angle from the corresponding point to its horizon in direction of the sun). A point is considered to be in the shadow of a nearby object if the sun lies below the horizon of the corresponding point. It is also assumed that those points casting a shadow are of a defined size (e.g. 0.3 m that is similar to the mean footprint diameter within the area). Consequently, points being closer to the current point have a greater influence (i.e. affect a wider range of azimuth angles) than those points being distant. Points being reflected from e.g. birds, lanterns etc. (i.e. such points have no neighbors in a defined search distance) are not considered for the calculation of the 3D horizon. Otherwise single points would cast shadows like high objects. Details of this procedure are described in Jochem et al. (2009b).

Shadows casted by the surrounding terrain are not considered directly. They are included in the CSI. This is due to the fact that the meteorological station is also affected by such shadows. The CSI - defined as the ratio of the observed and the modeled global radiation (Section 4.1) - is computed by modeling the global radiation on a horizontal surface close to the meteorological station. The CSI is computed for every single day of the year.

Calculation of the incoming solar radiation

The annual incoming solar radiation is calculated for each point of the 3D point cloud separately. It is calculated for each day of the year from sunrise till sunset in hourly steps. Shadowing effects of nearby objects are checked by comparing the current elevation angle of the sun with the minimum required solar elevation angle for the current azimuth direction. If the considered point is affected by such shadows, its direct radiation is set to zero and only the diffuse component is computed. Atmospheric effects as well as shadowing effects of the terrain are considered by multiplying the CSI value of the corresponding day with the corresponding sum of the daily global solar radiation. As a result the annual global solar radiation of each point within the study area is calculated.

Merging of Tiles

As the whole dataset is divided into several subareas for processing (Section 3.2) merging of the single tiles is a required step in order to get information about the incoming solar radiation for the whole study area. Merging of tiles is performed by writing the computed values of the incoming global solar radiation of each point back to the database (Section 2.2) . Optionally, the results can also be stored as a SAGA *Point Cloud* dataset (i.e. the results of each tile are stored separately). The buffer areas do not have to be considered for the procedure of merging. They are only required to avoid edge effects when calculating features such as slope and aspect as well as the 3D horizon of each point.

5 Results and Discussion

In this section the results of the point feature calculation and of the point cloud based solar radiation model are presented and discussed.

Calculation of slope and aspect

As mentioned in Section 3.3 the point based determination of slope and aspect depends on the normal vector of the orthogonal regression plane that is fitted to the point of interest and its 3D k nearest neighbors. The resultant normal vector on the point of interest is strongly influenced by the number of k nearest neighbors. Hence, a different number of k nearest neighbors might lead to different values of slope and aspect, respectively, at some locations. This is illustrated in Figure 3. The slope of ridged roofs is calculated by setting $k = 10$ and $k = 27$, respectively. As one can see a value of $k = 27$ results in a more homogeneous distribution of the calculated slope values within the different parts of a roof (ridge, roof planes) meaning that the noise within these parts is suppressed. The challenge is to find an appropriate value of k. Therefore, the calculated slope values of points on roof planes are inspected visually because roof planes are assumed to be planar facets (if not disturbed by e.g. chimneys, dormers etc.) and to be characterized by equal inclination and aspect angles. In this study the value of k is set to 27 to calculate both slope and aspect of each point.

Using a fixed number of k nearest neighbors instead of a fixed search distance for feature calculation leads to the consequence that the neighborhood (spatially seen) is adjusted to the different point densities within the test site. The different point densities are caused by overlapping flight strips and changing airplane attitude. However, this procedure leads to an extended neighborhood in areas characterized by very low point densities. This increases the probability that points reflected from locations having different properties of inclination are used for the calculation of slope and aspect. In such areas smoothing of the surface might occur. Robust plane fitting for feature calculation as performed in e.g. Dorninger and Pfeifer (2008) results in almost identical normal vectors of points belonging to one segment (i.e. areas characterized by similar slope and aspect angles such as roof planes). Such plane fitting algorithms are capable to handle a high noise level and are robust in areas of intersecting segments. This means that the occurrence of changing normal vectors on e.g. roof ridges would be suppressed.

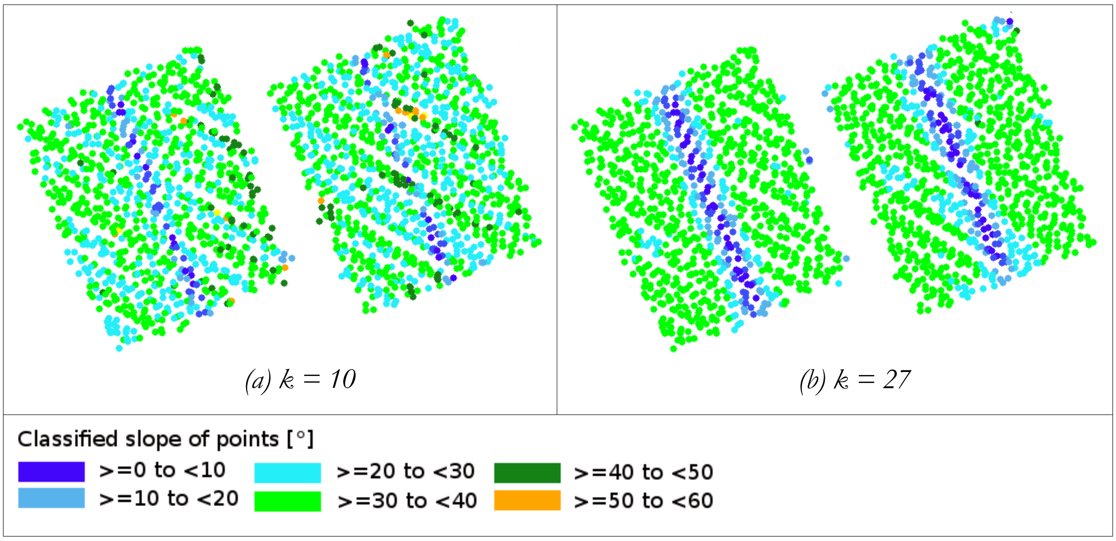

Fig. 3: Slope of points on ridged roofs is calculated by using a different number of 3D k nearest neighbors.

Dividing the whole dataset into several subareas is required to overcome the limitations of the computer 's main memory. The buffer areas surrounding each tile guarantee a proper selection of the *k* nearest neighbors of points being close to the edge of a subarea. Otherwise the calculation of slope and aspect of such points would result in falsified values and in the occurrence of edge effects.

Solar radiation modeling

The presented solar radiation model uses the full 3D information of the point cloud for both modeling of the incoming solar radiation and the calculation of the 3D horizon of each point. Using a normalized Digital Surface Model (nDSM) to calculate shadow masks of objects would suffer from a proper consideration of 3D shapes such as roof overhangs, chimneys etc. due to rasterization of the point cloud. Selected results of the presented solar radiation model are shown in Figure 4. The right column considers and the left column does not consider shadows of nearby objects. By modeling the shadows within the point cloud the strong local gradients of the incoming solar radiation can be modeled in a more detailed way. Areas that are affected by shadows of nearby objects (e.g. vegetation, buildings) receive less solar energy than those areas not being influenced by shadows of nearby objects. In this study transparent properties of vegetation are not considered. Shadows caused by vegetation are considered as being shadows of a solid non-transparent object. Taking the transparent properties of vegetation into account requires the classification of the point cloud into transparent and non-transparent objects in advance. This is performed in e.g. Jochem et. al (2009b).

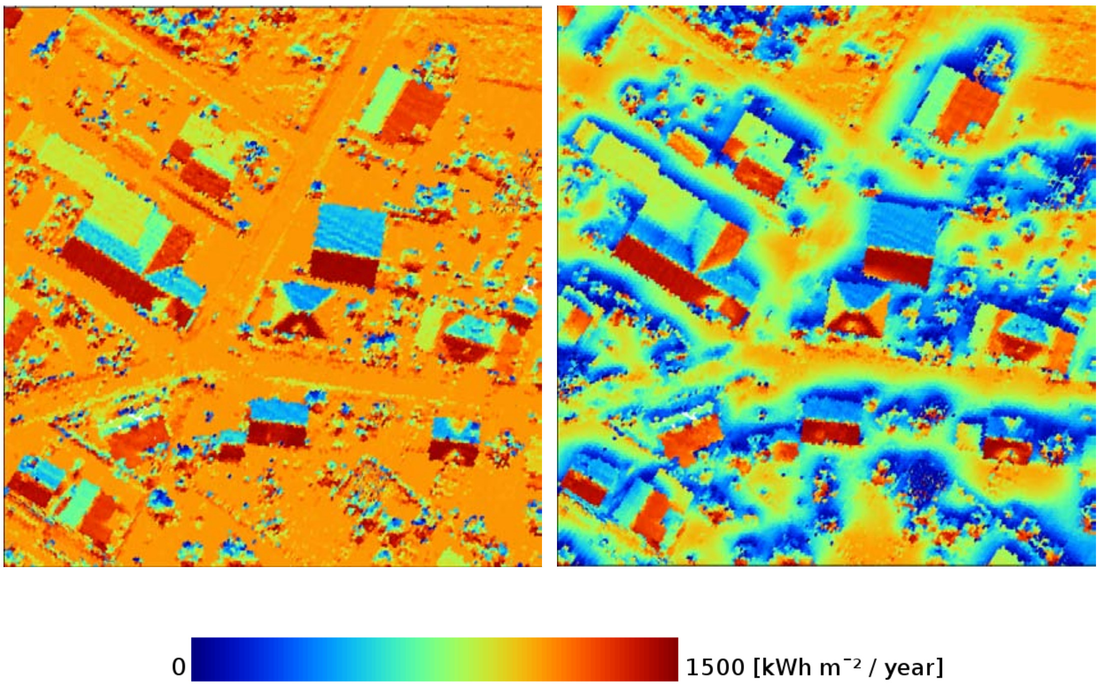

Fig. 4: Results of point cloud based solar radiation modeling. Left: incoming solar radiation without considering shadows of nearby objects. Right: consideration of shadows caused by objects by calculating the horizon of each point within the original 3D point cloud.

The CSI is used in both cases to correct the modeled solar radiation values and to take atmospheric and shadowing effects of the surrounding terrain into account. This procedure might lead to failures at locations that are influenced by atmospheric or shadowing effects, which do not influence the meteorological ground station. Improvements could be made by having data from several meteorological stations distributed within the research area. Hence, the CSI could be taken from that station, which is closest to the location the global incoming solar radiation is calculated for.

6 CONCLUSION AND OUTLOOK

In this paper a point cloud based solar radiation model, which is completely embedded into Open Source SAGA GIS is presented. It uses the full 3D information of the point cloud for both modeling of the incoming solar radiation and of the 3D horizon of each point. In order to handle the huge amount of point cloud data with limited computer memory the whole point cloud dataset is stored in a Laser data Information System based on a PostgreSQL/PostGIS database. This allows seamless data access and thus facilitates tile based processing within SAGA GIS. Combining the presented workflow with grid computing enables the possibility of spatial parallelization of the geoprocessing steps and to accomplish high processing performance (e.g. Lanig and Zipf 2008). The usage of buffer areas surrounding each tile is required to ensure a proper selection of *k* nearest neighbors when calculating point features such as slope and aspect. Furthermore, the buffer areas are also required when modeling shadowing effects of nearby objects within the point cloud. Solar radiation modeling based on point clouds acquired by e.g. ALS Systems allows for a proper consideration of the strong local gradients in the incoming solar radiation because (i) the 3^{rd} dimension is taken into account and (ii) 3D shapes are represented in a more correct way. Merging of tiles is accomplished by writing the values of the incoming global solar radiation calculated for each point back to the Laserdata Information System.

Future studies will concentrate on (i) parallelization of the geoprocessing tasks by means of grid computing and on (ii) segmentation and classification of the point cloud into solid and transparent objects on large areas. This allows high perfomance point cloud based solar radiation modeling by taking the transparent properties of vegetation into account.

ACKNOWLEDGEMENTS

The authors would like to thank the Federal State of Vorarlberg for supplying the LiDAR data.

REFERENCES

DORNINGER, P., PFEIFER, N., (2008): A COMPREHENSIVE AUTOMATED 3D APPROACH FOR BUILDING EXTRACTION, RECONSTRUCTION, AND REGULARIZATION FROM AIRBORNE LASER SCANNING POINT CLOUDS. - SENSORS 8(11), 7323-7343.

FU, P., RICH, P.M. (1999): DESIGN AND IMPLEMENTATION OF THE SOLAR ANALYST: AN ARCVIEW EXTENSION FOR MODELING SOLAR RADIATION AT LANDSCAPE SCALES. - IN: PROCEEDINGS OF THE 19TH ANNUAL ESRI USER CONFERENCE. SAN DIEGO, USA.

FU, P., RICH, P.M. (2002): A GEOMETRIC SOLAR RADIATION MODEL WITH APPLICATIONS. – IN: AGRICULTURE AND FORESTRY. COMPUTERS AND ELECTRONICS IN AGRICULTURE, 37(1-3), 25 - 35.

HE, Y. (2010): A SEGMENT-BASED APPROACH FOR DIGITAL TERRAIN MODEL DERIVATION IN AIRBORNE LASER SCANNING DATA. - MASTER THESIS. ENSCHEDE, THE NETHERLANDS: INTERNATIONAL INSTITUTE FOR GEO-INFORMATION SCIENCE AND EARTH OBSERVATION.

HOFIERKA, J., ŠÚRI, M. (2002): THE SOLAR RADIATION MODEL FOR OPEN SOURCE GIS: IMPLEMENTATION AND APPLICATIONS.- IN: PROCEEDINGS OF OPEN SOURCE GIS - GRASS USERS CONFERENCE 2002. TRENTO, ITALY.

HÖFLE, B. (2007): DETECTION AND UTILIZATION OF THE INFORMATION POTENTIAL OF AIRBORNE LASER SCANNING POINT CLOUD AND INTENSITY DATA BY DEVELOPING A MANAGEMENT and analysis system. - Dissertation. Innsbruck, Austria: Faculty of Geo- and Atmospheric Sciences, University of Innsbruck.

Jochem, A., Höfle, B., Rutzinger, M., Pfeifer, N. (2009a): Automatic roof plane detection and analysis of airborne LiDAR point clouds for solar potential assessment. - Sensors, 9(7), 5241-5262.

Jochem, A., Höfle, B., Hollaus, M., Rutzinger, M. (2009b): Object detection in airborne LiDAR data for improved solar radiation modeling. - In: IAPRS, XXXVIII (3/W8). Laserscanning 2009. Paris, France.

Kassner, R., Koppe, W., Schüttenberg, T., Bareth, G. (2008): Analysis of the solar potential of roofs by using official lidar data. – In: IAPRS. Beijing, China, pp. 399 - 403.

Lanig, S., Zipf, A. (2009): Interoperable processing of digital elevation models in grid infrastructures.- Earth Science Informatics (2009), 107-116.

Ludwig, D., Lanig, S., Klärle, M.(2009): Towards Location-based Analysis for Solar Panels by High Resolution Remote Sensors (LiDAR). - In ICC2009. 24th International Cartography Conference. Santiago. Chile.

Mount, D. M., Arya, S. (1997): ANN: a library for approximate nearest neighbor searching. In: Proceedings of the second annual center for geometric computing workshop on computational geometry, electronic edn., Durham, NC, USA, (http://www.cs.duke.edu/CGC/workshop97.html).

Myers, D.R. (2003): Solar Radiation Modeling and Measurements for Renewable Energy Applications: Data and Model Quality. – In: International Expert Conference on Mathematical Modeling of Solar Radiation and Daylight-Challenges for the 21st Century. Edinburgh, Scotland.

NREL (2002): NREL 2000 - SOLPOS documentation, National Renewable Energy Laboratory, Center for Renewable Energy Resources Renewable Resource Data Center.

Petrini-Monteferri, F., Wichmann, V., Georges, C., Diego, M., Stötter, J. (2009): Erweiterung der GIS Software SAGA zur Verarbeitung von Laserscanning-Daten der Autonomen Provinz Bozen Südtirol. - In: J. Strobl, T. Blaschke, & G. Griesebner (Eds.): Angewandte Geoinformatik 2009, Beiträge zum 21. AGIT-Symposium.

Pons, X., Ninyerola, M. (2008): Mapping a topographic global solar radiation model implemented in a GIS and refined with ground data. - International Journal of Climatology, 28, 1821–1834.

Rieger, W., Seebacher, M., Würländer, R., Bauerhansl, C. (2005): Erstellung eines Laser-DHM für Vorarlberg 2002 bis 2005. – In: Chesi/Weinold (Eds.): Internationale Geodätische Woche Obergurgl 2005, Tagungsband. Heidelberg: Wichmann-Verlag, pp. 115 - 124.

Šúri, M., Hofierka, J. (2004): A new GIS-based solar radiation model and its application to photovoltaic assessments. - Transactions in GIS, 8(2), 175 - 190.

Vögtle, T., Steinle, E., Tóvári, D. (2005): Airborne laserscanning data for determination of suitable areas for photovoltaics. – In: IAPRS. Enschede, The Netherlands, pp. 215-220.

Wehr, A., Lohr, U. (1999): Airborne laser scanning an introduction and overview. - International Journal of Photogrammetry and Remote Sensing, 54, 68-82.